

## Sedimentary porewaters record regional tectonic and climate events that perturbed a deep-sea brine pool in the Gulf of Aqaba, Red Sea

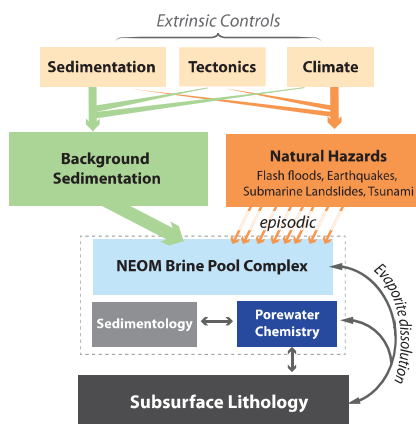
Gaëlle Duchâtelier<sup>\*</sup>, Amanda M. Oehlert<sup>\*</sup>, Hannah Shernisky, Clément G.L. Pollier, Peter K. Swart, Bolton Howes, Sam J. Purkis

*Department of Marine Geosciences, Rosenstiel School of Marine, Atmospheric and Earth Science, University of Miami, Miami, FL 33149, USA*

### HIGHLIGHTS

- Porewater chemistry influenced by turbidity currents that frequently disturbed NEOM Brine Pool
- Perturbations by regional tectonic and climatic events are recorded in porewater chemistry.
- Porewater records from deep-sea brine pools provide insight into timing and frequency of natural disasters.
- Brine pools are dynamic environments that host life at the edge of habitability.

### GRAPHICAL ABSTRACT



### ARTICLE INFO

Editor: Christian Herrera

**Keywords:**  
Brine Pool  
Geochemistry  
Porewaters  
Turbidites  
Gulf of Aqaba, Red Sea

### ABSTRACT

Brine pools in deep-sea environments provide unique perspectives into planetary and geological processes, extremophile microbial communities, and sedimentary records. The NEOM Brine Pool Complex was the first deep-sea brine pool system found in the Gulf of Aqaba, representing a significant extension of the geographical range and depositional setting of Red Sea brine pools. Here, we use a combination of brine pool samples collected via cast using a conductivity, temperature, depth instrument (CTD), as well as interstitial porewaters extracted from a sediment core collected in the NEOM Brine Pool to characterize the chemical composition and subsurface evolution of the brine. New results indicate that the NEOM brines and the subsurface porewaters may originate from different sources. Elemental concentrations suggest the brines in the NEOM pool are likely derived from dissolution of sub-seabed evaporites. In contrast, the sedimentary porewaters appear to have been influenced by periodic turbidite flows, generated either by earthquakes, submarine landslides, or flash floods, in which normal marine waters from the overlying Red Sea became entrained, periodically disturbing the chemistry of the brine pool. Thus, sediment porewaters beneath brine pools may record transient and dynamic changes in these deep marine depositional environments, reflecting the interplay between climate, tectonics, and sedimentation patterns along a rapidly urbanizing coastline. In concert, new results from NEOM extend the range and chemical

\* Corresponding author at: 4600 Rickenbacker Causeway, Miami, FL 33149, USA.

E-mail address: [aohlert@miami.edu](mailto:aohlert@miami.edu) (A.M. Oehlert).

constraints on Red Sea Brine Pools and highlight the dynamic interplay between Red Sea Deep water, dissolving evaporites, turbidites, and subsurface fluids that produce these unique depositional environments which host microbial life at the edge of habitability. In concert with sedimentological indicators, the chemistry of porewaters beneath deep-sea brine pools may present detailed records of natural hazards arising from interactions between the atmosphere, lithosphere, hydrosphere, and anthroposphere.

## 1. Introduction

Brine pools are dense bodies of highly saline water, or brine, that form lake-like structures in seafloor depressions (Ross and Hunt, 1967). Brine pools have been found in the Gulf of Mexico, the Mediterranean Sea, and the Red Sea (Antunes et al., 2011; Camerlenghi, 1990; Cita, 1991; Cita, 2006; Joye et al., 2005; MacDonald et al., 1990; Shokes et al., 1977; Wallmann et al., 1997; Westbrook and Reston, 2002; Yakimov et al., 2013; Purkis et al., 2022a; Herut et al., 2022). The formation of these deep-sea ecosystems has been attributed to a number of different factors and processes such as (1) the dissolution and seepage of evaporitic deposits in sediment layers below water bodies through salt tectonics, (2) the heating and dissolution of salts by hydrothermal fluids associated with hotspots and tectonic spreading centers, (3) dissolution of locally exposed evaporites, or (4) relic brine pools (Vengosh and Starinsky, 1993; Vengosh et al., 1998; Augustin et al., 2018; Cita, 2006; Hunt et al., 1967; Censi et al., 2019; Salem, 2017). The high salinity of brine seeping from the seafloor makes the water dense compared to the surrounding seawater, allowing the brine to accumulate in depositional lows.

Throughout the 1960s, the Red Sea central rift zone was intensively investigated due to the discovery of anomalous temperatures, high salinities, and the discovery of two brine pools: the Atlantis II Deep and the Discovery Deep which are attributed to hydrothermal formation (Backer and Schoell, 1972; Gurvich, 2006; Reysenbach and Cady, 2001; Schmidt et al., 2003; Swallow and Crease, 1965). Following this discovery, at least 25 brine pool systems in total have been discovered within the Red Sea (Backer and Schoell, 1972; Batang et al., 2012; Duarte et al., 2020; Miller et al., 1966; Pautot et al., 1984; Purkis et al., 2022a). Red Sea brine pool complexes have previously been categorized based on the temperature, depth, and geological setting of the pools: hot, deep-sea brine pools are located within the axial trough of the Red Sea Rift while cool brine pools are located in shallower depths in close proximity to the shoreline (Anschutz et al., 1999; Antunes et al., 2011; Backer and Schoell, 1972; Batang et al., 2012; Cochran et al., 1986; Duarte et al., 2020; Gurvich, 2006; Purkis et al., 2022a, 2022b; Table S1). The hot axial brine pools are characterized by anoxic conditions and water temperatures that are substantially warmer than ambient seawater due to hydrothermal activity associated with the basin's spreading axis (Anschutz et al., 1999; Ross and Hunt, 1967; Schardt, 2016). The cool, coastal brine pools, meanwhile, consist of two brine pools located on the shallow coastal shelf offshore of Saudi Arabia away from the axial trough: the Thuwal Seeps at 860 m deep (Batang et al., 2012) and the Afifi Brine Pool at 350 m deep (Duarte et al., 2020). These two anoxic pools both contain hypersaline waters that are not substantially warmer than ambient seawater, thus making them cold compared to the axial pools.

Geochemical analysis of the brine pools has also proven useful in the classification of brine pool complexes. Red Sea brine pools have also been classified as Type I or Type II brine pools based on their geochemistry and interpreted origin (Schmidt et al., 2015; Table S1). According to this classification scheme, Type I brine pools are typically located off-axis from the central rift, and their brine chemistry is controlled by evaporite dissolution and sediment alteration, indicated by patterns in the concentrations of  $\text{Na}^+$ ,  $\text{K}^+$ ,  $\text{Br}^-$ ,  $\text{Cl}^-$ , and  $\text{SO}_4^{2-}$  (Schmidt et al., 2015). These brine complexes are characterized by high salinity, low pH, low temperatures, and low trace metal concentrations, indicating that hydrothermal fluids are of minor importance when

considering influences on brine origin. In contrast, Type II brine pools are strongly influenced by hydrothermal fluids from interactions between seawater and volcanic rock due to proximity to the central rift. Type II brine pools are characterized by high concentrations of elements such as Mn, Fe, and Zn and lower concentrations of Mg and  $\text{SO}_4^{2-}$  attributed to hydrothermal fluids (Schmidt et al., 2015).

The discovery of the NEOM Brine Pool represents the first brine pool to be found in the Gulf of Aqaba, and the only brine pool discovered outside of the Red Sea central basin (Purkis et al., 2022a). NEOM differs compared to other pools in that it is located only 2 km from shore, 10× closer to the shoreline than the next closest cool-coastal brine pool (Thuwal Seeps, ~25 km from shore; Batang et al., 2012). Situated at an abyssal depth of 1770 m, the NEOM Brine Pool and its surrounding environment also host exceedingly rich microbial fauna and metazoan assemblages, providing insight into life at its most extreme (Purkis et al., 2022a). Quantitative characterization of microbial communities in brine pools with different classifications may provide insight into the habitability and tolerance ranges of extremophiles analogous to those that arose on early Earth. While the NEOM Brine Pool can likely be classified as a cool, shore-proximal brine pool based on temperature and location of discovery (Purkis et al., 2022a), the data in-hand preclude classification as either a Type I or Type II brine pool (*sensu* Schmidt et al., 2015). Given the limited examples of Type I brine pools that currently exist in the literature, classification of the NEOM Brine Pool could potentially provide only the third confirmed Type I brine pool complex in the greater Red Sea Region, accompanying pools such as Oceanographer (Backer and Schoell, 1972; Anschutz et al., 1999) and Kebrit (Backer and Schoell, 1972), and providing insight into the dynamics of extremophiles in low temperature pools with hypersaline and anoxic conditions. Although much progress has been made in characterizing the composition of brine pools, especially the axial brine pool associated with hydrothermal activity in the central Red Sea over the past decades, the elemental composition of porewaters from sediments beneath such brine pools are also understudied in the region. Interstitial porewaters potentially represent an important archive of information regarding the origin and evolution of these brine pools. While analysis of sediment porewaters has been conducted in a core collected from the Atlantis II Deep Brine Pool (Anschutz et al., 2000), a Type II Brine Pool *sensu* Schmidt et al. (2015), to our knowledge sedimentary porewaters have yet to be studied in any of the Type I Brine Pools.

Complimenting scientific interest in brine pools as early Earth analogues, sedimentological records from beneath the NEOM brine pool indicate exceptional preservation of a detailed record of geological hazards impacting human civilization over the past ~1200 years (Purkis et al., 2022a, 2022b). The tectonic setting and morphology of the Red Sea make it uniquely susceptible to multiple geological hazards, including earthquakes, submarine landslides, and tsunami resulting from the fault-controlled morphology of the basin (Ben-Avraham et al., 1979; Ben-Avraham, 1985; Shaked et al., 2004; Salem, 2009; Kanari et al., 2015; Goodman Tchernov et al., 2016; Ash-Mor et al., 2017; Purkis et al., 2022a). The narrow width of the Gulf of Aqaba further amplifies impacts of tsunami in the region, because there is little opportunity for energy dispersion before arriving to coastal zones (Purkis et al., 2022b). Further climate-controlled impacts on sedimentation include changes in grain size associated with prolonged periods of drought in the adjacent desert regions (Kalman et al., 2020) and flash floods which can produce significant hyperpycnal gravity flows transporting terrigenous sediment to the deep (Katz et al., 2015; see their

Fig. 3 and their Video S1 for excellent example). Deposits induced by turbidity currents and submarine landslides have previously been observed in brine pools from the Red Sea (Botz et al., 2007), Mediterranean (Stanley and Maldonado, 1981; Rimoldi, 1993; Rimoldi et al., 1996), and the Gulf of Mexico (Sawyer et al., 2019), demonstrating the anoxic and highly saline conditions characteristic of brine pools around the world likely promote unique and exceptional preservation of the archive of geological hazards in Earth history. In the vicinity of the Gulf of Aqaba, regional urbanization and growing infrastructure projects, including residential districts, tourist resorts, and other facilities, demonstrate the need for understanding of the timing, frequency, and impact of such geological hazards (Chalastani et al., 2020).

Here, our aim is to analyze the geochemistry of the brine pool waters and porewaters extracted from sediments directly underlying the NEOM Brine Pool to provide insight into the origin and evolution of the brine pool using the Schmidt et al. (2015) brine pool classification scheme (Type I vs Type II). We hypothesize that these new datasets will provide insight into perturbations experienced by the NEOM brine pool, and results will contribute to the developing record of natural hazards in the region. In addition to previously reported measurements of temperature,  $\text{Na}^+$ ,  $\text{Cl}^-$ , and total sulfur concentrations (Purkis et al., 2022a), we present new measurements of elemental composition, especially  $\text{Mg}^{2+}$ ,  $\text{Ca}^{2+}$ , B, and  $\text{Li}^+$  concentrations, as well as  $\text{Mg}/\text{Ca}$  ratios in both the brine pool itself, as well as new interstitial porewaters extracted from a sediment core collected from the bed of the pool. Results provide new insight into the chemical processes occurring in this environment, permitting an evaluation of plausible origins of the NEOM Brine Pool and the influence of perturbations produced by natural hazards such as flash floods, tsunamis, earthquakes, and submarine landslides that impact the anthroposphere, atmosphere, hydrosphere, and lithosphere.

## 2. Materials and methods

### 2.1. Depositional setting and sample collection

The geological and environmental conditions of the Red Sea have promoted the formation of extreme environments that may provide insight into the conditions of early Earth. The Red Sea began forming about 30 Ma when the Arabian Plate started rifting from the African Plate (Coleman, 1993; McGuire and Bohannon, 1989). The onset of this

rift transitioned the spreading center from a continental rift to an oceanic rift and led to more extensive fault activity associated with volcanism at 24–23 Ma (Bosworth, 2015; Bosworth and Burke, 2005; Stockli and Bosworth, 2018). Existing tectonic models of the Red Sea are variable and contradictory with respect to the extent and age of seafloor spreading, locations of faults, and distributions of ocean crust in the Red Sea Basin. However, a recent model argues that continuous seafloor spreading began at least 12–13 Ma along the central rift, making the present-day Red Sea a fully mature ocean basin that has completed its rifting phase (Purkis et al., 2012; Augustin et al., 2021). Hydrothermal sediments and alteration of magmatic rock are associated with this area of active seafloor spreading along the central Red Sea rift (Scholten et al., 2000). At the start of rifting around the beginning of the Miocene, evaporites were deposited across the central Red Sea, with deposits containing halite beds and other evaporites with mixed lithologies of halite, anhydrite, shales, carbonates, and clastic sediments (Hughes and Beydoun, 1992). The hydrothermal sediments and evaporite deposits associated with the Red Sea basin have created unique source rock materials that facilitate the development of extreme marine environments such as anoxic submarine brine pools.

The Gulf of Aqaba is located in the easternmost bifurcation of the northern Red Sea (Fig. 1). Approximately 180 km long and 8 km wide, the Gulf of Aqaba is a deep terminal elongated basin reaching a maximum depth of 1829 m (Ibrahim and Abdelmenam, 2013). The NEOM Brine Pool, named after a 2020 research cruise sponsored by NEOM and the OceanX “Deep Blue”, is the first brine pool discovered in the Gulf of Aqaba (Purkis et al., 2022a). This brine complex consists of one large brine pool and three minor pools located within 50 m of the main pool. The NEOM Brine Pool is 260 m long, 70 m wide, and has an area of 10,000  $\text{m}^2$ , while the minor pools are circular and have areas of <10  $\text{m}^2$  (Purkis et al., 2022a). The NEOM Brine Pool sits at an abyssal depth of 1770 m, and although it is much deeper than the Thuwal Seeps and Afifi Brine Pool, NEOM brines have similarly cool temperatures (~21.8 °C; Purkis et al., 2022a). Of all the brine pools of the Red Sea region, NEOM is the most shore-proximal pool, situated just 2 km offshore from the coast (Purkis et al., 2022a).

Cast data from a conductivity, temperature, depth instrument (CTD, Sea-Bird 011+) indicates that the water column above the brine pool had a salinity of 40 practical salinity units (PSU), a temperature of 21.33 °C, and dissolved oxygen of 180  $\mu\text{mol/L}$  (Purkis et al., 2022a).

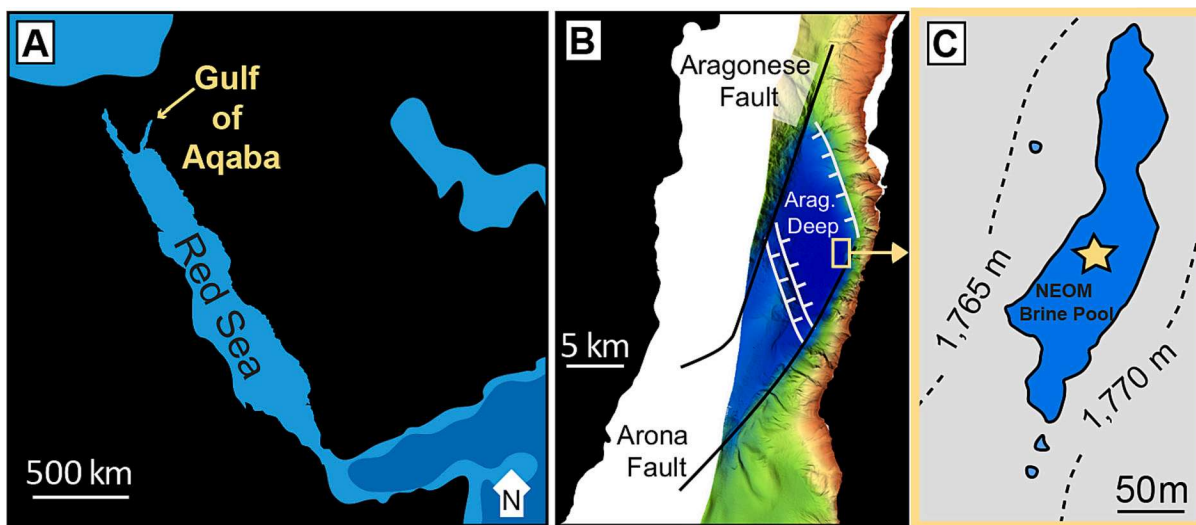


**Fig. 1.** Map of the location and tectonic setting of the NEOM Brine Pool Complex. A) Location of the Gulf of Aqaba, situated at the northernmost extent of the Red Sea. B) Shows the Aragonese Deep (abbreviated as Arag. Deep), which is bounded by Arona and Aragonese faults (black lines) within the Gulf of Aqaba. Cooler colors correspond to deeper depths. The NEOM Brine Pool Complex is located on the eastern margin of the Aragonese Deep (yellow box in B (modified from Purkis et al., 2022a)). C) Expanded view of the inset box in panel B, which shows the morphology of the NEOM Brine Pool Complex. The sediment core studied here was collected from the deepest portion of the pool, marked by a star in panel C (modified from Purkis et al., 2022a).

These parameters remained constant down to 1769.26 m deep until reaching the brine-seawater interface. The salinity of the brine 20 cm below the brine interface overwhelmed the conductivity probe at 120 PSU, and further laboratory-based analysis has revealed the true salinity of the brine to be 160 PSU (Purkis et al., 2022a). The dissolved oxygen content decreased to 50 µmol/L approximately 20 cm below the brine interface and reached a minimum of <10 µmol/L by 50 cm beneath the brine-seawater interface. Unlike salinity and dissolved oxygen, the temperature of the brine changed only slightly below the interface, creating a very small temperature increase of 1 °C in the brine pool compared to the overlying water column. The low dissolved oxygen values classify the NEOM Brine Pool as an anoxic environment, and the modest warming of the brine suggests a lack of hydrothermal influence on the pool (Purkis et al., 2022a). In a previous study, samples of the Red Sea seawater located 500 and 5 m above the brine pool, at the brine-seawater interface, and within the brine pool itself were collected using a 12 x 12 L rosette of Niskin bottles (Purkis et al., 2022a). Measurements of salinity, alkalinity, initial pH and the concentration of Na<sup>+</sup>, SO<sub>4</sub><sup>2-</sup>, and Cl<sup>-</sup> in the NEOM brine pool were previously reported using the same methods applied here (Purkis et al., 2022a).

Deployed from the OceanXplorer, a 6000 m-rated Argus Mariner XL remotely operated vehicle (ROV) was used to collect a 150 cm sediment core (CHRO017-5) in a PVC tube from the pool using the ROV's hydraulic manipulator arm. During coring, the sediments were compacted, and here we will report measurements relative to compacted depths in the collected core. Upon recovery, the core was capped on both ends and stored under refrigeration until its delivery to the Rosenstiel School of Marine, Atmospheric, and Earth Science. Previous work employing computerized tomography and sedimentological description indicated that this core contains a sedimentological record of at least ten grain-rich, siliciclastic turbidite sequences possibly generated by flashfloods and associated hyperpycnal flows, or through earthquake-initiated turbidites (Purkis et al., 2022a, 2022b).

## 2.2. Intersstitial porewater collection

Holes were drilled through the sediment core liners using a handheld power drill at sequential increments guided by observation of sedimentary structures related to compacted depth collected using a CT scan (Purkis et al., 2022a). Five-centimeter Rhizon samplers with silicone O-rings were inserted through the drill holes for porewater collection that leaves sedimentary record intact (Dickens et al., 2007). A 60-mL polypropylene syringe was connected via luer-lock to each Rhizon sampler to collect water samples extracted. Porewater extraction using Rhizons carries the advantage of filtration to 0.22 µm during collection, thus porewaters were filtered upon collection from microbial and colloidal contaminants (Dickens et al., 2007; Knight et al., 1998; Seeberg-Elverfeldt et al., 2005). Extracted porewaters ranged in volume from 5 to 15 cm<sup>3</sup>, likely related to downcore variations in sedimentology and permeability (Purkis et al., 2022a). Very little porewater was recovered in samples collected between 35 and 45 cm, and thus it was not possible to analyze these samples. After collection, porewaters were transferred to 50-mL centrifuge tubes, treated with 50 µL of concentrated ultratrace HNO<sub>3</sub>, and stored in a dark refrigerator prior to analysis.

## 2.3. Geochemical analyses

Both brine pool and porewater samples were gravimetrically diluted proportional to their salinity with 1 % nitric acid prepared with distilled nitric acid (Savillex Acid Purification system, DST-1000) and 18 MΩ MilliQ water (MilliQ7005) in a Class 100 UL 1805 certified polypropylene trace metal workstation in an ISO Level 7 Clean Room. Elemental concentrations were determined using triple quadrupoleinductively coupled plasma mass spectrometry (Agilent 8900, Agilent Technologies, Santa Clara, CA, USA) at the University of Miami, FL. The 8900 was equipped with an integrated autosampler (SPS-4) with

HEPA filtration and coverkit, Ni skimmer and sampler cones, and standard electron multiplier detector. In these analyses, a standard sample introduction system, including a glass MicroMist nebulizer, a quartz double pass spray chamber, and quartz torch with 2.5 mm id injector, and a UHMI setting of 8 was used for online sample dilution using Ar gas. Instrument operation was conducted in Mass Hunter 4.5 Workstation Software (C.01.05). Three replicate analyses consisting of 100 sweeps each were conducted for each measurement, and all reported values represent measurements with <10 %, but typically lower than 5 % RSD. For all elements, the instrument was operated in MS/MS mode in either No gas, He, H<sub>2</sub> and O<sub>2</sub> gas modes using the collision-reaction cell (CRC). Instrument tuning was conducted prior to each analysis, and the tuning solution contained 1 µg/g Li, Y, and Tl (Agilent Technologies Tuning solution) which allowed for the optimization of signal sensitivity and peak resolution at low, mid, and high *m/z* ranges as previously (Harouaka et al., 2021). Plasma-derived oxides and doubly charged ions were monitored before each analytical batch and maintained below 2 % and 3 %, respectively. Scandium and Indium were introduced using the Agilent online internal standard kit to serve as internal standards. National Research Council Canada (NRCC, Ottawa, Canada) seawater certified reference material (CRM) CASS-6 and International Association for the Physical Sciences of the Oceans (IAPSO) seawater were used for method validation and estimates of accuracy in repeat analyses with each analytical batch. A seven-point external calibration curve was produced from commercially available multi-element solutions produced by Agilent Technologies and was certified using NIST-traceable Spex Certiprep solutions and/or CRMs (IAPSO and CASS-6), both with reproducibility better than ±10 %. Following convention of Duarte et al. (2020), data are reported in mM in data tables below. For comparison to Red Sea datasets presented by Schmidt et al. (2015), data were converted to mg/L. Chloride concentrations were measured by titration with 0.1 M silver nitrate using a solution of potassium permanganate and potassium di-chromate as an end-point indicator and calibrated using IAPSO seawater Gieskes et al. (1991). Data analysis, including preparation of ternary diagrams, was conducted in Geochemist's Workbench 12.0.

Alkalinity was measured using a Gran titration method (Gran, 1950) in which increments of 0.1 M HCl acid were added to between 5 and 10 cm<sup>3</sup> of filtered porewater using a computer interfaced to Metrohm auto burette. As a result of the relationship between the change of pH, sample volume, and the quantity of acid needed to reach a pH of <2, the titration alkalinity can be calculated (Gieskes et al., 1991). The initial pH of the titration is taken as the pH of the pore fluid. The measurement is calibrated using solutions provided by Dickson et al. (2003) and provides a precision of <0.1 mM.

## 3. Results

### 3.1. NEOM Brine Pool

Geochemical analysis of the NEOM Brine Pool and overlying seawater in the Gulf of Aqaba revealed that the NEOM Brine Pool is an Na-Cl brine, with Na<sup>+</sup> and Cl<sup>-</sup> concentrated by a factor of ~4 relative to the overlying seawater of the Gulf of Aqaba (Table 1, Purkis et al., 2022a).

In addition, NEOM Brine Pool is enriched in K<sup>+</sup>, Ca<sup>2+</sup>, and Sr<sup>2+</sup> by factors >10 (Table 1). Concentrations of Mg<sup>2+</sup> and SO<sub>4</sub><sup>2-</sup> in the NEOM brine were lower than predicted by conservative behavior, with concentration factors < 4, which were the concentration factors for Na<sup>+</sup> and Cl<sup>-</sup> concentrations in the brine pool relative to the overlying seawater (Table 1). The Sr<sup>2+</sup> concentrations in the NEOM Brine Pool were enriched by a factor of ~30 in the brine pool. Boron and magnesium concentrations in the NEOM Brine Pool were 3.3 mM and 170 mM respectively. The concentration of Ca<sup>2+</sup> in the NEOM Brine Pool was 109 mM, and the molar ratio of magnesium to calcium in NEOM was 0.95.

**Table 1**

Elemental concentrations in NEOM Brine Pool (1760 m) and Gulf of Aqaba (1260 m). Concentrations reported previously by Purkis et al. (2022a) are denoted by an asterisk.

Element	NEOM brine	Gulf of Aqaba seawater	Brine/SW ratio
Na <sup>+</sup> (mM)	2350*	565*	3.9
Cl <sup>-</sup> (mM)	2780*	685*	4.1
Mg <sup>2+</sup> (mM)	170	61	2.8
K <sup>+</sup> (mM)	59	6	10.7
Ca <sup>2+</sup> (mM)	109	9	10.7
Total S (mM)	10*	35*	0.3
Sr <sup>2+</sup> (mM)	3	0.1	30.2
B (mM)	3.3	1.0	3.3
Li <sup>+</sup> (mM)	0.142	0.035	4.1

### 3.2. Sedimentary porewaters

Major cation and anion concentrations of sedimentary porewaters collected from CHR0017–5 are reported in Table S2, and excess plots are shown in Fig. 2. Like the overlying brine, sedimentary porewaters were dominated by Na<sup>+</sup> and Cl<sup>-</sup>, which ranged from 1428.5 to 2018.4 mM and 2281.8 to 3126.6 mM respectively. The Mg<sup>2+</sup> concentrations varied from 112.6 to 180.2 mM, while Ca<sup>2+</sup> ranged from 52.3 to 98.9 mM. Boron (B) concentrations ranged from 1.7 to 2.9 mM in the porewaters, K<sup>+</sup> from 12.31 to 15.23 mM, and total S from 7.46 to 15.61 mM. Lithium (Li) concentrations ranged from 51.4 to 81.6 μM. Stratigraphic variation in porewater composition was explored using ionic concentration vs depth and ‘excess plots’ (Fig. 2), where porewater values were normalized to those in the NEOM Brine Pool adapted from calculations presented by Swart and Kramer (1998). Chloride, a conservative ion, exhibited concentrations lower than the overlying brine pool at shallow depths, and concentrations that exceeded that of the brine pool at 25 to 30 cm depth (Fig. 2). Small relative increases in Cl<sup>-</sup> were also observed

in porewaters collected from the base of the core. Overall, concentrations of K<sup>+</sup>, Mg<sup>2+</sup>, Ca<sup>2+</sup>, Sr<sup>2+</sup>, total boron (Fig. 2) were lower in the porewaters than in the NEOM Brine Pool. Concentrations of Mg<sup>2+</sup> exhibited stratigraphic variability with measurements at 30 cm and between 60 and 85 cm characterized by excess values in the porewaters that exceeded those of the overlying brine pool (Fig. 2). Total sulfur concentrations in the porewaters were typically higher than those of the overlying brine pool in the upper section of the core until a depth of ~50 cm, beneath which porewater exhibited negative excess values (Fig. 2). Excess total alkalinity in the porewaters ranged from +1 to +2.5 mM relative to the brine pool (Fig. 2). Increases in excess alkalinity were observed between 60 and 80 cm, concurrent with increases in excess Mg<sup>2+</sup> concentrations (Fig. 2).

## 4. Discussion

### 4.1. Origin and classification of the NEOM Brine Pool

The NEOM Brine Pool contains Na-Cl brines that are approximately four times more saline than the overlying seawater in the Gulf of Aqaba (Purkis et al., 2022a). Comparison of the major element composition of the NEOM Brine Pool samples with published values for other Red Sea brine pools (Bonatti et al., 2005; Pätzold et al., 2000, 2003; Schmidt et al., 2011, 2013, 2015) revealed that the water type classification of all other pools can also be described as Na-Cl brines.

To compare other element concentrations in brines through the Red Sea, we converted our mM to mg/L as reported by Schmidt et al. (2015). Boron and magnesium concentrations in the NEOM Brine Pool were the second highest ionic concentrations relative to measurements conducted in other Red Sea brines (Schmidt et al., 2015; Anschutz et al., 2000), with the highest concentrations of boron (49.7 mg/L) and magnesium (6821 mg/L) found in Oceanographer Deep. The concentration of Ca in

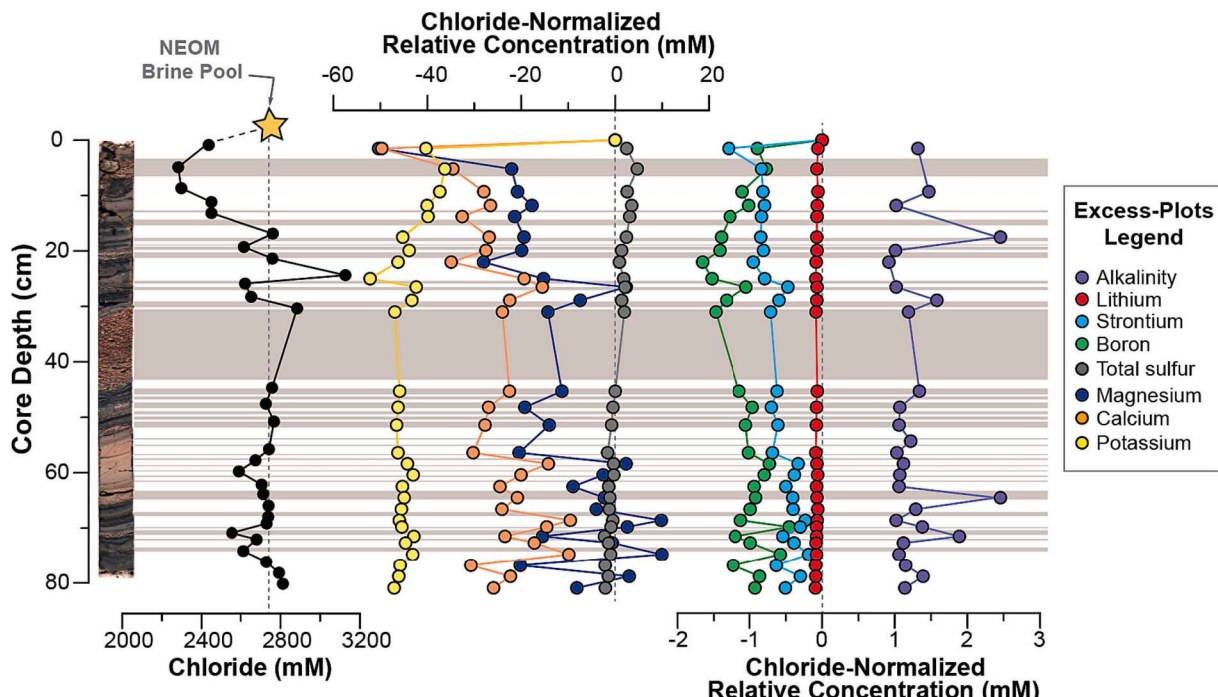


**Fig. 2.** Down-core trends in porewater composition. (Left to right) High resolution core photo is from Purkis et al., 2022a. Chloride concentrations are shown as black circles, with the orange star at the top of the plot showing the composition of the NEOM Brine Pool measured from CTD cast. Next, excess plots of chloride-normalized ions, including Mg<sup>2+</sup>, Ca<sup>2+</sup>, total Sulfur, K<sup>+</sup>, and finally, Sr<sup>2+</sup>, total boron, and total alkalinity in mM relative to the overlying NEOM Brine Pool composition, which is defined as zero (indicated by vertical dashed grey lines). Calculations were conducted following equations presented in Swart and Kramer (1998). Intervals highlighted in brown boxes across the plot represent coarse grained intervals in the core photo, including siliciclastic turbidites identified previously by Purkis et al. (2022a). Inadequate recovery volume of porewater from the thickest turbidite interval (~30 to 45 cm depth) precluded geochemical analyses in this section.

the NEOM Brine Pool was close to the average calcium concentration of other Red Sea brine pools (3310.2 mg/L), and the ratio of magnesium to calcium in NEOM was 0.95, most comparable to the Mg/Ca ratios of the Port Sudan (1.21), Erba (1.46) and Kebrat (1.3) brine pools (Fig. 4).

Ternary diagrams comparing the concentration of  $\text{Ca}^{2+}$ ,  $\text{Mg}^{2+}$ , and  $\text{SO}_4^{2-}$  in the NEOM Brine Pool to other Red Sea brine pools (Bonatti et al., 2005; Pätzold et al., 2000, 2003; Schmidt et al., 2011, 2013, 2015) revealed three groups of brine pools (Fig. 3), including: 1) a group containing Albatross, Nereus, Atlantis II, and Discovery which are characterized by relatively high  $\text{Ca}^{2+}$ , low  $\text{Mg}^{2+}$  and high  $\text{SO}_4^{2-}$  concentrations, 2) a second group of brine pools including Suakin, Port Sudan, Erba, Conrad, and Afifi which are characterized by low  $\text{Ca}^{2+}$ , high  $\text{Mg}^{2+}$ , and high  $\text{SO}_4^{2-}$  concentrations, and finally, 3) a third group which includes Kebrit, Oceanographer, and NEOM Brine Pools, which can be characterized by relatively high  $\text{Mg}^{2+}$ , low  $\text{Ca}^{2+}$  and low  $\text{SO}_4^{2-}$  concentrations (Fig. 3B). When  $\text{Ca}^{2+}$ ,  $\text{Mg}^{2+}$ , and  $\text{K}^+$  are compared in ternary diagrams, two groups of brine pools are differentiated (Fig. 3), including: 1) a group containing Nereus, Albatross, Discovery, and Atlantis II which are characterized by high  $\text{Ca}^{2+}$ , low  $\text{Mg}^{2+}$ , and high  $\text{K}^+$  concentrations, and 2) a group including Suakin, Port Sudan, Erba, Conrad, Afifi, Oceanographer, Kebrit, and NEOM which can be characterized by low  $\text{Ca}^{2+}$ , high  $\text{Mg}^{2+}$ , and low  $\text{K}^+$  (Fig. 3B).

Historically, the origin of many brine pools in the Red Sea have been attributed to the interaction of Red Sea water with evaporites in the sediment column that are likely Miocene in age (Craig, 1969; Schoell and Faber, 1978). More recent conceptual models, which classify brine pools (*sensu* Schmidt et al., 2015; Duarte et al., 2020) by their chemistry, aim to differentiate brine pools by the range of depositional settings, ambient brine temperatures, and major element chemistry. Analysis of the NEOM Brine Pool chemistry, including Mg/Ca ratios and elemental concentrations (B,  $Mg^{2+}$ ,  $SO_4^{2-}$ ,  $Ca^{2+}$ ,  $K^+$ ), indicate that the NEOM Brine Pool composition is a Type I brine pool, most comparable to the Kebrit and Oceanographer brine pools (Fig. 5, Table S3 Bonatti et al., 2005, Pätzold et al., 2000, 2003). The chemistry of these brine pools is controlled by the original Miocene salt deposit composition (Schoell and Faber, 1978) and fluids interacting with sedimentary strata that migrate from depth into the brine and change the original evaporite solution chemistry (Schmidt et al., 2015). Second to the Oceanographer brine pool, NEOM has the highest measured concentrations of boron and magnesium (Table 4). Brine rich in magnesium could be explained by the dissolution of Mg-rich evaporite minerals (Stoffers and Kühn, 1974) and/or the dissolution of detrital carbonaceous material (Pierret et al.,

2001), both of which would be accompanied by an increase in Ca, Sr, and dissolved inorganic carbon, as well as an increase in K concentration in the case of Mg-rich evaporite dissolution (Schmidt et al., 2015). The boron concentration of NEOM (35.9 mg/L) paired with the Mg/Ca ratio (0.95) of NEOM is most similar to that of Oceanographer and Kebrit (Table 4, Fig. 4). Published datasets for Suakin, Port Sudan, Conrad, Valdivia, and Erba suggest that these pools can be differentiated from NEOM, Kebrit, and Oceanographer by their relatively higher sulfate concentrations (Figs. 3, 4), despite similarly cool temperatures (see Fig. 1 from Purkis et al., 2022a). Thus, it may be expected that higher concentrations of sulfide minerals could be found in relatively low sulfate brine pool settings like NEOM, Kebrit, and Oceanographer, and potentially, greater abundances of sulfur-metabolizing microbial

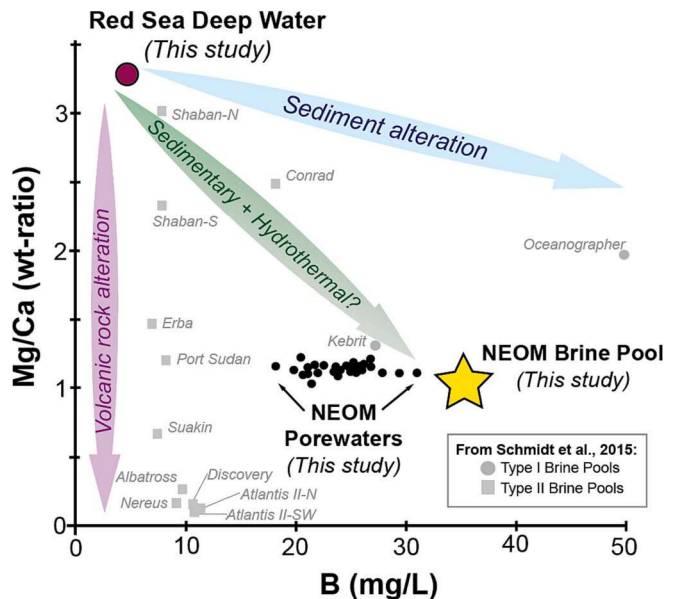


**Fig. 4.** Plot of boron concentrations (mg/L) vs. Mg/Ca ratios following notation of Schmidt et al. (2015), adapted to include Red Sea Deep Water (maroon circle), NEOM Brine Pool (yellow star), and sedimentary porewaters (black circles), measured in this study. Grey symbols represent published compositions of brine pools from Schmidt et al. (2015).

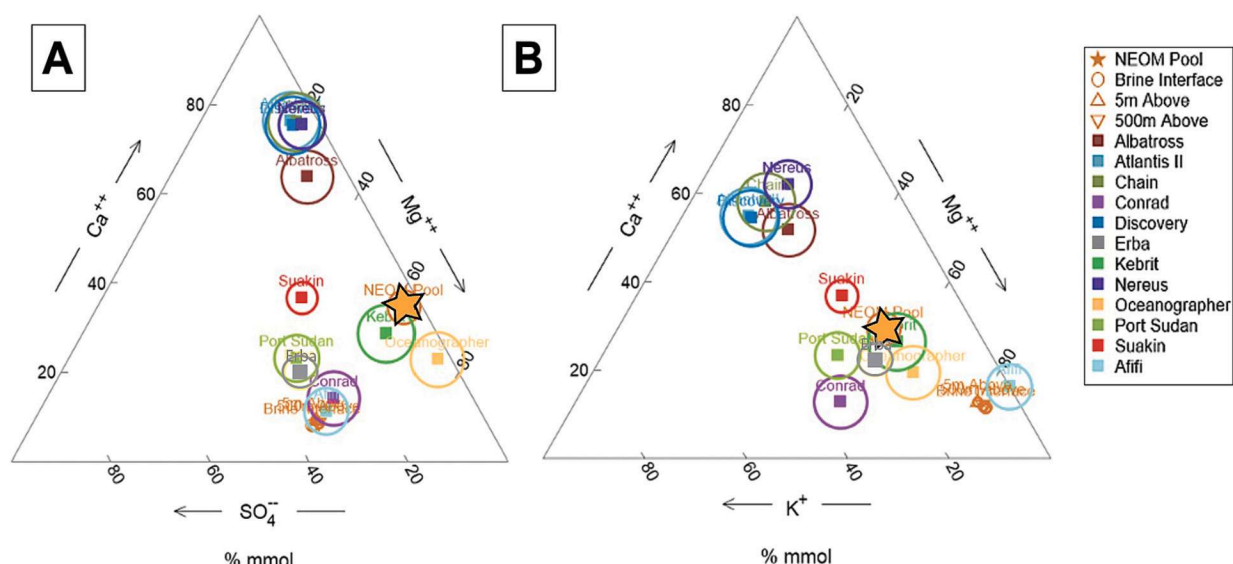


**Fig. 3.** (A) Ternary diagram of  $\text{Ca}^{2+}$ ,  $\text{Mg}^{2+}$ , and  $\text{SO}_4^{2-}$  of the Red Sea brine pools. (B) Ternary diagram of  $\text{Ca}^{2+}$ ,  $\text{Mg}^{2+}$ , and  $\text{K}^+$  concentrations in the Red Sea brine pools. The orange star shows the NEOM Brine Pool composition.

communities (Michaelis et al., 1990; Scholten et al., 2000; Trüper, 1969; Purkis et al., 2022a). Unlike NEOM, the Type 2 brine pools contain relatively lower boron concentrations, and plot along the geochemical pathway describing brine sources originating from volcanic rock alteration as proposed by Schmidt et al. (2015) (Fig. 4). Classification of the NEOM Brine Pool as Type I in this conceptual framework suggests that the chemistry of the NEOM brine pool is predominantly controlled by subsurface evaporite dissolution and contributions from sediment alteration, not alteration of volcanic materials as observed in Type II pools (Schmidt et al., 2015). These observations suggest that the origin and evolution of the NEOM brines have been impacted by processes like water-rock interaction, diagenesis, mineral dissolution (especially evaporites) and precipitation, and/or influences of microbial metabolisms similar to those occurring in the Kebrat and Oceanographer brine pools (Schmidt et al., 2015).

Measurements conducted on brine samples from the NEOM Brine Pool are consistent with conservative salinity enrichment, driven by increases in  $\text{Na}^+$  and  $\text{Cl}^-$  (Table 1). However, not all measured elements in the NEOM Brine Pool behave conservatively (Table 1). Concentrations of  $\text{Ca}^{2+}$  and  $\text{K}^+$  are approximately 10 times higher in the NEOM Brine Pool than in the seawater above, and  $\text{Sr}^{2+}$  concentration is 30 times higher, while total sulfur and  $\text{Mg}^{2+}$  enrichment factors are lower than expected (0.3 and 2.8, respectively), each of which are anomalous in comparison with other brine pools in the Red Sea. Elements that are relatively enriched relative to  $\text{Na}^+$  and  $\text{Cl}^-$  will be discussed in the context of possible explanations, followed by elements that were found to be depleted in the brines relative to the overlying Gulf of Aqaba seawater.

Enrichment of elements in brine pools has been observed in other brine pools of the Red Sea (Table S3), including the Atlantis II Deep brine pool complex (Zierenberg and Shanks, 1986; Anschutz and Blanc, 1995), Thuwal Seeps (Batang et al., 2012), as well as the Afifi brine pool (Duarte et al., 2020). Like NEOM, geochemical analyses of the Atlantis II Deep brine pool complex also exhibited enriched  $\text{Sr}^{2+}$  concentrations relative to the overlying normal Red Sea seawater, however, they were only enriched by a factor of ~4–6 (Zierenberg and Shanks, 1986; Anschutz and Blanc, 1995). In Atlantis II Deep, comparison of  $\text{Sr}^{2+}$  concentrations to radiogenic strontium isotopes ( $^{87}\text{Sr}/^{86}\text{Sr}$  values) and sediment mineralogy led the authors to conclude that  $\text{Sr}^{2+}$  was released during the dissolution of manganese- and iron-oxide minerals to form more stable forms of goethite, hematite, manganite, or todorokite (Anschutz and Blanc, 1995) supporting links between dynamic changes in sediment mineralogy during diagenetic reactions. Enrichment factors for many metals in the Thuwal Seeps brine pool system were found to be significantly higher than normal marine seawater, ranging from 10 to >140, despite having the lowest reported salinity values for brine pools in the Red Sea (Batang et al., 2012). In the Afifi brine pool, conservative enrichment of many of the major ions was observed by a factor of ~5.6, but elements like Fe, Mn,  $\text{PO}_4$ , and  $\text{SiO}_2$  exhibited non-conservative behavior and exceed these enrichment factors relative to the overlying seawater (Duarte et al., 2020). However, non-conservative enrichment in the Afifi Brine Pool occurs by smaller factors than those observed in our dataset from NEOM (Table 1). Interpreted to be similar to the Kebrat and Oceanographer brines, the Afifi brine pool was described to form via the mixing of Red Sea waters with formation waters impacted by the dissolution of underlying evaporitic sediments, rather than a hydrothermal origin (Duarte et al., 2020). Unfortunately, boron concentrations and  $\text{Mg}/\text{Ca}$  ratios were not reported for several of these systems, precluding the inclusion of the Afifi and Thuwal Seeps brine pools into the conceptual model of Type I and II brine pools presented by Schmidt et al. (2015) (Fig. 4). However, other geochemical indicators led the authors to conclude that the origin of the brines in Afifi was similar to Kebrat and Oceanographer (Duarte et al., 2020). Thus, it could be inferred that Afifi might also be a Type I brine pool like NEOM, while Thuwal Seeps has been alternatively interpreted to originate from an extant cold hydrocarbon seep site (Batang et al., 2012).

Both total S and  $\text{Mg}^{2+}$  concentrations and enrichment factors in the NEOM Brine Pool were lower than predicted by comparison to conservative elements like  $\text{Na}^+$  and  $\text{Cl}^-$  (Table 1), suggesting a process that preferentially removes these elements from the brine pool. Overall, concentrations of total sulfur in the NEOM Brine Pool were relatively low (~10 mM) compared to other brines in the Red Sea, which range from 8.5 mM at Chain to 72.0 mM at Valdivia (Backer and Schoell, 1972; Karbe, 1987; Pierret et al., 2001) as well as sulfate concentrations in normal marine seawater (28 mM; Canfield and Farquhar, 2009). In the NEOM Brine Pool, sulfur enrichment factors are lower than expected (0.3) considering conservative behavior of other elements in the brine (Table 1). Low concentrations of sulfur in the brine pool itself (inferred to be present as sulfate in oxidized environments, and hydrogen sulfide in anoxic settings) support the interpretation of high rates of microbial sulfate reduction and sulfide oxidation in the anoxic waters of the NEOM pool (Purkis et al., 2022a). Brine pool chemistry in the greater Red Sea has also been characterized to have low sulfate concentrations, such as in Atlantis II (Anschutz et al., 2000), where halotolerant sulfate-reducing microbial communities have been isolated from the seawater-brine interface (Trüper, 1969), as well as in Kebrat Deep, which was shown to contain high concentrations of  $\text{H}_2\text{S}$  (a product of microbial sulfate reduction (Hartmann et al., 1998)) and minerals formed with reduced sulfur like pyrite and sphalerite (Michaelis et al., 1990; Scholten et al., 2000). Shaban Deep, another brine pool occurring in a water depth of 1325 m, was found to have massive sulfide deposits and  $\text{H}_2\text{S}$ -free anoxic brines (Michaelis et al., 1990), as well as isotopic evidence of biogenic sulfate reduction in the form of  $\delta^{34}\text{S}$  values enriched in  $^{34}\text{S}$  (Blum and Puchelt, 1991). In contrast to our data from the NEOM pool, sulfate concentrations from the Afifi brine pool indicate a similar enrichment factor as major elements like  $\text{Na}^+$  and  $\text{Cl}^-$  suggesting that metabolisms contributing to biogeochemical cycling of sulfur were not important in this environment (Duarte et al., 2020). In a controlled experiment investigating the development of biofilms in the vicinity of Thuwal Seeps, Lee et al. (2014) measured sulfate in the pool waters (2.9 g/L or 26.9 mM), but comparison of enrichment factors for  $\text{Cl}^-$  (2.8) and sulfate (1.03), as well as genetic identification of sulfate-reducing bacteria indicate some degree of sulfate reduction in the Thuwal Seeps.

#### 4.2. Origin of downcore changes in the chemistry of sedimentary porewaters

Sedimentary porewaters exhibited significant downcore changes in chemistry, with some intervals characterized by less saline porewaters, and others by more saline brines. Variations in key elements occurred with depth, especially those related to carbonate and evaporite minerals (Figs. 2, 4, 5). Chloride, which does not actively participate in sediment diagenetic reactions, provides important insight into the origin and evolution of the porewaters (Fig. 2). Chloride concentrations in the porewaters varied with depth (Fig. 2), indicating that salt was added, or water was removed in different proportions through time (i.e., Zhang, 2020). Relative depletions in  $\text{Cl}^-$  can occur from the addition of waters with lower salinity through time. One plausible explanation may be entrainment of shallower Red Sea water within the first, shallow siliciclastic rich turbidite that was deposited in the upper part of the core (Fig. 2, see Purkis et al., 2022a). Many of the grain-rich turbidites, including ten turbidite intervals identified previously within the core (Purkis et al., 2022a) are similarly associated with decreased concentrations of  $\text{Cl}^-$  (Fig. 2). At approximately 60 cm depth, another interval of porewaters with low  $\text{Cl}^-$  concentrations was observed, and associated with several thin, coarse-grained intervals (Fig. 2). Porewater  $\text{Cl}^-$  concentrations are as much as 17.3 % lower than the overlying Brine Pool, especially in the upper 13 cm of the core (Fig. 2). Red Sea Deep Water, which is characterized by a  $\text{Cl}^-$  concentration of 684.7 mM at a depth of ~1200 m (Purkis et al., 2022a), may have been entrained by periodic coarse-grained turbidity currents. Previous work supports this interpretation—hyperpycnal flows have been shown to entrain fresher waters

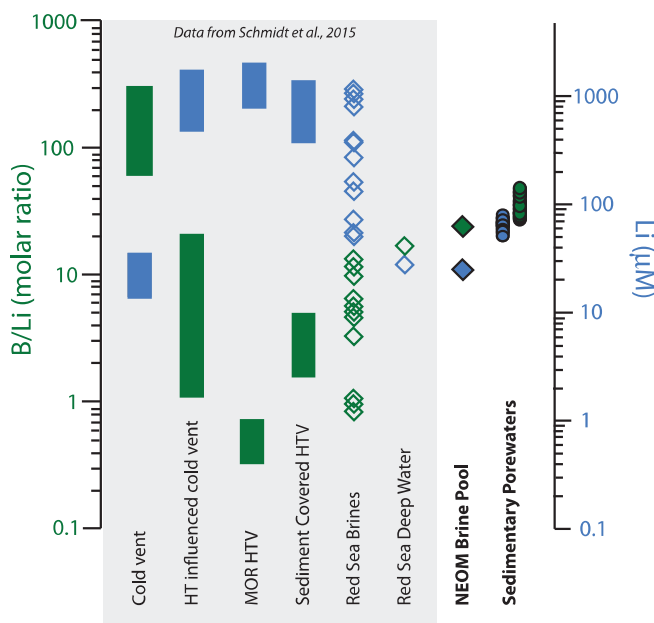


**Fig. 5.** Plots of B/Li (molar ratio) and Li ( $\mu\text{M}$ ). Green symbols show B/Li, blue symbols show Li concentration. NEOM Brine Pool samples are shown as filled diamonds, and sedimentary porewaters are shown as filled circles. Data from Schmidt et al. (2015) are shown in grey box using the same abbreviations: Hydrothermal (HT), Mid Ocean Ridge Hydrothermal Vent (MORHTV), Hydrothermal Vent (HTV).

from flash floods to the offshore environments (Katz et al., 2015). Thus, we hypothesize that the disruption of the brine pool by turbidity currents (Purkis et al., 2022a) can be preserved in both the lithological composition of the cores, as well as the porewater chemistry. The frequent coarse-grain flows arriving to the NEOM Brine Pool that occurred over the past ~1200 years (Purkis et al., 2022a) have significantly impacted the sedimentology and the chemistry of the NEOM Brine Pool periodically—a signature that appears to have been propagated to the porewater archive over time. Consequently, porewater geochemistry of sediments beneath Red Sea brine pools may represent a rich and understudied archive that document turbidite-driven hydrochemical changes to this environment induced by regional changes in climate, tectonics, and sedimentation.

On the other hand,  $\text{Cl}^-$  concentrations can also be relatively enriched compared to the brine pool in some sedimentary layers, including those at depths between 25 and 30 cm, and 35 cm (Fig. 2). Relative enrichments in  $\text{Cl}^-$  can occur through several mechanisms, first, increased brine seepage rates from the toe-of-slope that enhance the proportion of saline brines delivered to the low, second, entrainment of hypersaline brines originating from sabkhas located adjacent to shallow marine environment via flash floods and/or turbidity currents, or third, through the removal of water during diagenetic alteration of ash and hydrous diagenetic minerals (Martin, 1994; Torres et al., 1995; Zhang, 2020). To differentiate the various mechanisms that impact porewater chemistry associated with such perturbations, further analysis of brine chemistry and porewaters, coupled with detailed geochemical and petrographic analyses of the sediments seeking to identify ash and terrigenous sediment layers in these intervals, is warranted. For instance, previous studies have shown that compositional changes in sediment grain-size and metal-to-silica ratios can provide insight into the frequency and intensity of flash flood events in the past (i.e., Katz et al., 2015).

Analysis of the Mg/Ca ratios and boron concentrations using the Schmidt et al. (2015) conceptual framework further support the interpretation that the porewaters may be the result of mixing of two sources of waters (Fig. 4). The first brine source would be the overlying NEOM Brine Pool, which we interpret to have formed as a result of dissolution

of sedimentary evaporites and sediment-water interactions, classified as a Type I pool in the conceptual model of Schmidt et al. (2015). Consistent with the geochemical classification, photographic evidence of brines seeping from the toe-of-slope on the eastern Gulf of Aqaba was recovered during the submersible dives from the OceanXplorer that recovered the sediment core studied here (Purkis et al., 2022a, see their Fig. 5). The second source is characterized by lower boron concentrations and B/Li ratios compared to the brine pool itself (Fig. 5), as well as other brine pools reported by Schmidt et al. (2015). Entrainment of shallower waters by turbidity currents, as described above, is one possibility. A second possibility is the lateral migration of brines into the porewaters that were previously influenced by volcanic rock alteration, indicated by the shift towards lower boron concentrations in the porewaters at depth (Figs. 2, 4). Concentrations of Li and molar ratios of B/Li provide additional support for this interpretation (Fig. 5). The B/Li molar ratios were higher in the NEOM Brine Pool and porewaters than in the Red Sea Deep Water. In concert with changes in  $\text{Cl}^-$ , these observations suggest that the relative balance of brines, including those seeping out from the slope, those delivered by turbidity currents, and those potentially migrating into the system laterally, likely changed through the evolutionary history of the brine pool.

In general, study of the geochemical composition of interstitial porewaters extracted from other Red Sea brine pool sediment cores remains underexplored. In comparison to the composition of metalliferous sediment porewaters extracted from the Atlantis II Deep (Anschatz et al., 2000), the porewaters in the sediment core from NEOM Brine Pool typically have significantly lower average elemental concentrations for  $\text{Ca}^{2+}$ ,  $\text{Na}^+$ ,  $\text{K}^+$ , and  $\text{Cl}^-$ . Porewaters from NEOM have on average  $\sim 4.8 \times$  elevated  $\text{Mg}^{2+}$  compared to those measured from Atlantis II Deep (Anschatz et al., 2000). These differences can likely be attributed to dissimilar geological settings and origins of these brine pools. The Atlantis II Deep and characteristic metalliferous sediments represent an active hydrothermal system in the Red Sea with hot fluids feeding into an axial depression (Anschatz and Blanc, 1995; Hartmann et al., 1998), which can explain lower concentrations of elements such as  $\text{Mg}^{2+}$  and boron. In the NEOM porewaters, concentrations of  $\text{Mg}^{2+}$  were higher than the overlying brine at core depths of 26.5, 58.4, 68.6, 69.8, 74.8, and 78.8 cm. When increases in  $\text{Mg}^{2+}$  are coupled with increases in the concentrations of  $\text{Ca}^{2+}$ ,  $\text{Sr}^{2+}$ , and alkalinity, Mg-rich carbonate mineral dissolution is likely occurring (Swart and Kramer, 1998). The decrease in excess sulfur in the porewaters beneath 48.2 cm may be explained by sulfate reduction (Swart and Kramer, 1998) in the core (Fig. 2), which can initially produce corrosive porewaters facilitating carbonate mineral dissolution (i.e., Mackenzie and Andersson, 2011).

#### 4.3. Implications for extreme environments and early earth

Deep sea brine pools present one of the most extreme habitable environments on Earth. Brine pools are characterized by high osmotic stress, anoxia, high hydrostatic pressure, and low water activity yet still support unique microbial communities of extremophiles demonstrating life at its most extreme (Antunes et al., 2011; Joye, 2020; Fisher et al., 2021). An important characteristic of these anoxic hypersaline basins is the formation of salinity, temperature, density, and oxygen gradients at the seawater-brine interface above the pool that prevents the mixing of oxidants, reductants, and organic or inorganic particulate matter able to support microbial cell growth (Antunes et al., 2020). The distinct chemical compositions of deep sea hypersaline anoxic brines have been referred to as ‘isolated islands of evolution’ due to high genetic novelty, distinct microbial communities, and the prevention of cross-colonization among individual pools attributable to salinity, ion composition, and anoxia (Stoeck et al., 2014).

Continued discovery of new deep sea brine pools provides opportunity for discovering new taxa that may potentially exist in such unknown environments (Fisher et al., 2021), with high potential for biotechnological application development like anticancer therapeutics (Ziko et al.,

2019; Esau et al., 2019). Prior research on Red Sea Brine pools suggested that Type I brine pools were relatively rare, and case studies were limited to Kebrat (Pätzold et al., 2000, 2003) and Oceanographer (Bonatti et al., 2005). With the discovery of the NEOM Brine Pool (Purkis et al., 2022a) and the new insights into its chemical composition presented here, there is an opportunity to more deeply investigate differences in the composition and metabolic function of the microbial communities that are found in these distinct chemical environments. 16S rRNA sequencing of microbial communities associated with sediments in the upper 20 mm beneath the NEOM Brine Pool indicate that anaerobic prokaryotes, including sulfate reducers, are the predominant communities associated with this environment (Purkis et al., 2022a). Our results suggest that the chemistry of shore-proximal brine pools like NEOM can be periodically impacted by geological hazards that perturb otherwise stable extreme conditions established by their abyssal location. Consequently, such geological hazards may exert a selective influence on the genetic composition of the communities that inhabit such environments. Comparative investigations of the genetic range of microbial communities associated with the modern brine pool and perturbed intervals is warranted.

Primordial life was suggested to have originated in anoxic and hypersaline conditions, approximately 1.5 to 2 times more saline than modern ocean salinity (Knauth, 1998; Knauth, 2005; Knoll, 2015; Dundas, 1998), suggesting that the brine pools like NEOM which have been discovered in the Red Sea, Mediterranean, and Gulf of Mexico may provide a modern analogue for the conditions that fostered life as we know it (Mancinelli et al., 2004; van der Wielen et al., 2005). More than two decades of research indicates that study of extreme environments, like the deep hypersaline brine pools, can more precisely delineate the limits of life (Horikoshi, 1998; Javaux, 2006; Javor and Javor, 1989; Rothschild and Mancinelli, 2001) and provide well constrained analogues that aid in the study of depositional settings targeted in the search for life on Mars. For example, studies of brine-driven diagenesis of clay minerals on Earth include Lake Lewis (English, 2001); the Pleistocene Lake Tecopa (Larsen, 2008); the Tyrell Basin, Australia (Macumber, 1992), and other saline lakes (Deocampo and Jones, 2014), each of which have provided key case studies for comparison of the recently collected *in situ* measurements collected by the Curiosity Rover exploring the Gale Crater on Mars (Bristow et al., 2021). Thus, a multitude of chemical, microbiological, medical, and geological questions motivate continued study of these extreme environments.

#### 4.4. Implications for reconstructing the frequency of geological hazards to coastal communities

Our results indicate that both brine pool sediments and their associated porewaters can record changes in the frequency and intensity of deposits produced by natural hazards such as flash floods, earthquakes, tsunami, and submarine landslides which can produce turbidity currents. Interplay between sedimentation, tectonics, and climate can produce normal background sedimentation, as well as punctuated episodes of perturbation, including natural hazards like tsunami, earthquakes, submarine landslides, and flash floods (Fig. 6). The ability to attribute turbidites in brine pool sequences to a particular origin will be an important step in refining timescales for these natural hazards (Fig. 6, orange arrows). Enhanced understanding of the frequency of flash floods versus earthquakes, submarine landslides, and tsunami is essential to develop strategies that protect rapidly growing coastal communities and infrastructure (Chalastani et al., 2020). Multiple cascading threats, including submarine landslide-tsunamis generated by an earthquake are a particular concern (Salamon et al., 2021). Even an incipient landslide in the Tiran Strait has been implicated in the generation of a 10 m tsunami wave (Purkis et al., 2022b). We suggest that consideration of sedimentary evidence in tandem with coeval porewater chemistry may provide additional information regarding turbidite origin. For instance, turbiditic episodes induced by flash floods should be expected to entrain

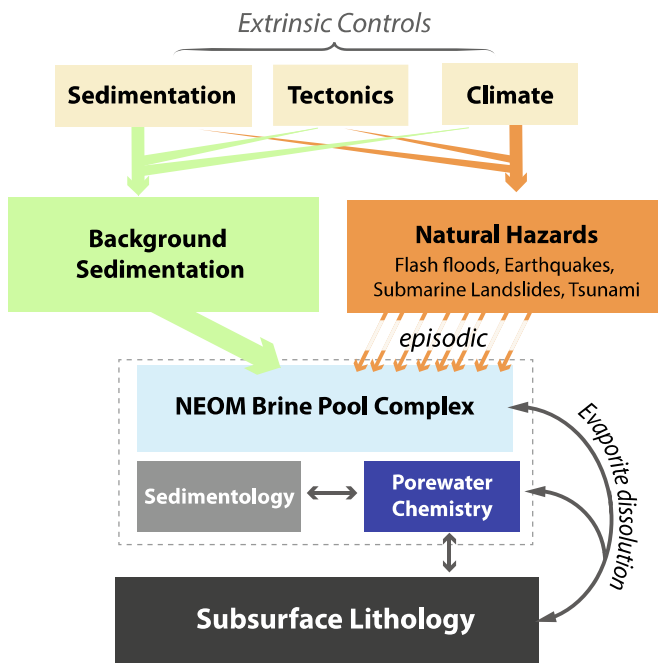


**Fig. 6.** Schematic representation of factors that impact porewater chemistry in the NEOM brine pool, including connections between extrinsic controls, including sedimentation, tectonics, and climate occurring as a consequence of background processes versus episodic natural hazards (flash floods, earthquakes, landslides, and tsunami) and subsurface lithology.

lower salinity waters than submarine processes. Conversely, submarine landslides or earthquakes may entrain water with chemistry more like shallow marine conditions of the Red Sea, entrained within anomalously old sediment packages containing shallow marine allochems (Ash-Mor et al., 2017). Further high-resolution sedimentological and geochemical analysis of intervals characterized by porewaters with low  $\text{Cl}^-$  may provide key indicators of which geological hazard is responsible for each event layer.

Eventually, diffusion will attenuate the unique porewater signatures (i.e., Blättler et al., 2019), associated with deposition induced by geological hazards, thus, it should be expected the relative depletions and enrichments of porewater chemistry are a transient phenomenon, potentially providing insight into only geologically recent dynamics of water sources and perturbations. Nonetheless, attributing changes in porewater chemistry is expected to provide longer-term insight into societal risks from geological hazards, increasing the record from decades (i.e., Cramer et al., 2018) to centuries or even millennia (Kalman et al., 2020; Purkis et al., 2022a). Comparison of sedimentology and porewater chemistry of brine pools across the entire Red Sea system could thus provide unprecedented insight into spatiotemporal dynamics of geological hazards occurring at the intersection of geological processes, climate, and society.

#### 5. Conclusions

Geochemical analysis of the NEOM Brine Pool and associated sedimentary porewaters have revealed two insights into the dynamics of these extreme environments at the base of the Gulf of Aqaba in the Red Sea. First, by applying the conceptual framework of Schmidt et al. (2015) our new results indicate that the NEOM Brine Pool is a Type I brine pool, likely produced through subsurface dissolution of evaporites flowing out onto the seafloor. Only the third Type I brine pool confirmed, this new observation prompts NEOM as a critical modern analogue for evaluating unique trends in extremophile microbial communities in Type I vs Type II brine pools and their role in economically

significant deposits of metals like Mn. Second, geochemical analysis of porewaters revealed a dynamic subsurface environment impacted by water-rock interactions and perturbations induced by turbidity currents. Low pH and total sulfur concentrations in the porewaters coincide with peaks in alkalinity and concentrations of  $\text{Ca}^{2+}$  and  $\text{Mg}^{2+}$  at the base of the core, suggesting active diagenetic regimes inducing dissolution of carbonate minerals. Low boron,  $\text{Cl}^-$ , and relatively high  $\text{Li}^+$  concentrations in the pore waters within turbidites in this core relative to the NEOM pool itself suggest that waters of lower salinity were delivered to the brine pool by flash floods or during episodic earthquakes/tsunami in the recent geological past. Thus, in addition to serving as pristine, undisrupted sedimentological archives preserved in an anoxic hypersaline environment with implications for early Earth and potentially Mars, the underlying sediments also appear to contain a detailed geochemical archive of societally-relevant geological hazards.

## Role of funding source

Start-up funds provided to A.M.O. by the Rosenstiel School of Marine, Atmospheric, and Earth Science supported these analyses.

## CRediT authorship contribution statement

**Gaëlle Duchatellier:** Data curation, Formal analysis, Investigation, Visualization, Writing – original draft, Writing – review & editing. **Amanda M. Oehlert:** Conceptualization, Data curation, Formal analysis, Investigation, Methodology, Project administration, Supervision, Visualization, Writing – original draft, Writing – review & editing. **Hannah Shernisky:** Data curation, Formal analysis, Investigation. **Clément G.L. Pollier:** Formal analysis, Methodology, Writing – review & editing. **Peter K. Swart:** Conceptualization, Data curation, Formal analysis, Investigation, Methodology, Writing – review & editing. **Bolton Howes:** Formal analysis, Investigation, Writing – review & editing. **Sam J. Purkis:** Conceptualization, Data curation, Funding acquisition, Investigation, Methodology, Project administration, Writing – review & editing.

## Declaration of competing interest

The authors declare no competing interests.

## Data statement

All data that support the findings of this study are available in the main text or supplementary material.

## Acknowledgements

We owe a debt of gratitude to our Saudi Arabian partners, NEOM, and to Paul Marshall for facilitating the Deep Blue Expedition and issuing sampling permits. Francesca Benzoni, Fabio Marchese, and Giovanni Chimienti assisted with sampling and ideation of this study and we are similarly indebted to OceanX and the crew of OceanXplorer for their operational and logistical support for the duration of this expedition. In particular, we would like to acknowledge Mattie Rodriguez, Olaf Dieckhoff, Ewan Bason, Carmen Greto, and Colleen Peters for data acquisition, sample collection and support of scientific operations on board OceanXplorer. We would also like to thank OceanX Media for documenting and communicating this work with the public, as well as Morgan Chakraborty and Akos Kalman for discussions about sedimentology of the core. Finally, we are grateful to three anonymous reviewers for constructive feedback that improved this manuscript.

## Appendix A. Supplementary data

Supplementary data to this article can be found online at <https://doi.org/10.1016/j.scitotenv.2023.168804>.

<https://doi.org/10.1016/j.scitotenv.2023.168804>.

## References

- Anschutz, P., Blanc, G., 1995. Chemical mass balances in metalliferous deposits from the Atlantis II deep, Red Sea. *Geochim. Cosmochim. Acta* 59 (20), 4205–4218. [https://doi.org/10.1016/0016-7037\(95\)94444-k](https://doi.org/10.1016/0016-7037(95)94444-k).
- Anschutz, P., Blanc, G., Chatin, F., Geiller, M., Pierret, M.-C., 1999. Hydrographic changes during 20 years in the brine-filled basins of the Red Sea. *Deep-Sea Res. I Oceanogr. Res. Pap.* 46 (10), 1779–1792. [https://doi.org/10.1016/s0967-0637\(99\)0019-9](https://doi.org/10.1016/s0967-0637(99)0019-9).
- Anschutz, P., Blanc, G., Monnin, C., Boulègue, J., 2000. Geochemical dynamics of the Atlantis II Deep (Red Sea): II. Composition of metalliferous sediment pore waters. *Geochim. Cosmochim. Acta* 64, 3995–4006. [https://doi.org/10.1016/S0016-7037\(00\)00486-5](https://doi.org/10.1016/S0016-7037(00)00486-5).
- Antunes, A., Ngugi, D.K., Stingl, U., 2011. Microbiology of the Red Sea (and other) deep-sea anoxic brine lakes. *Environ. Microbiol. Rep.* 3 (4), 416–433. <https://doi.org/10.1111/j.1758-2229.2011.00264.x>.
- Antunes, A., Olsson-Francis, K., McGenity, T.J., 2020. Exploring deep-sea brines as potential terrestrial analogues of oceans in the icy moons of the outer solar system. *Curr. Issues Mol. Biol.* 38, 123–162. <https://doi.org/10.21775/cimb.038.123>.
- Ash-Mor, A., Bookman, R., Kanari, M., Ben-Avraham, Z., Almogi-Labin, A., 2017. Micropaleontological and taphonomic characteristics of mass transport deposits in the northern Gulf of Eilat/Aqaba, Red Sea. *Mar. Geol.* 391, 36–47. <https://doi.org/10.1016/j.margeo.2017.07.009>.
- Augustin, N., van der Zwan, F.M., Devey, C.W., van der Zwan, F.M., 2018. A modern view on the Red Sea Rift: tectonics, volcanism and salt blankets. In: *Geological Setting, Palaeoenvironment and Archaeology of the Red Sea*, pp. 37–52. [https://doi.org/10.1007/978-3-319-99408-6\\_3](https://doi.org/10.1007/978-3-319-99408-6_3).
- Augustin, N., van der Zwan, F.M., Devey, C.W., Brandsdóttir, B., 2021. 13 million years of seafloor spreading throughout the Red Sea Basin. *Nat. Commun.* 12 (1) <https://doi.org/10.1038/s41467-021-22586-2>.
- Backer, H., Schoell, M., 1972. New deeps with brines and metalliferous sediments in the Red Sea. *Nat. Phys. Sci.* 240 (103), 153–158. <https://doi.org/10.1038/physci240153a0>.
- Batang, Z.B., Papathanassiou, E., Al-Suwailem, A., Smith, C., Salomidi, M., Petihakis, G., Aliukunhi, N.M., Smith, L., Mallon, F., Yapici, T., Fayad, N., 2012. First discovery of a cold seep on the continental margin of the Central Red Sea. *J. Mar. Syst.* 94, 247–253. <https://doi.org/10.1016/j.jmarsys.2011.12.004>.
- Ben-Avraham, Z., 1985. Structural framework of the Gulf of Elat (AQABA), Northern Red Sea. *J. Geophys. Res. Solid Earth* 90 (B1), 703–726. <https://doi.org/10.1029/JB090iB01p00703>.
- Ben-Avraham, Z., Almagor, G., Garfunkel, Z., 1979. Sediments and structure of the Gulf of Elat (Aqaba)—Northern Red Sea. *Sediment. Geol.* 23 (1–4), 239–267. [https://doi.org/10.1016/0037-0738\(79\)90016-2](https://doi.org/10.1016/0037-0738(79)90016-2).
- Blättler, C.L., Higgins, J.A., Swart, P.K., 2019. Advection glacial seawater preserved in the subsurface of the Maldives carbonate edifice. *Geochim. Cosmochim. Acta* 257, 80–95.
- Blum, N., Puchelt, H., 1991. Sedimentary-hosted polymetallic massive sulfide deposits of the Kebrat and Shaban Deep, Red Sea. *Miner. Depos.* 26, 217–227.
- Bonatti, E., Bortoluzzi, G., Calafato, A., Cipriani, A., Ferrante, V., Ligi, M., Lopez Correa, M., Redini, F., Barabino, G., Caminati, E., Mitchell, N., Sichler, B., Schmidt, M., Schmitt, M., Rasul, N., Al Nomani, S., Bahareth, F., Khalil, S., Farawati, R., Gitto, D., Raspagliosi, M., 2005. Geophysical, Geological and Oceanographic Surveys in the Northern Red Sea. Report on the Morphobathymetric, Magnetometric, Oceanographic, Coring and Dredging Investigations During Cruise RS05 Aboard R/V *Urania*, p. 94.
- Bosworth, W., 2015. Geological evolution of the Red Sea: historical background, review, and synthesis. In: *The Red Sea*, pp. 45–78. [https://doi.org/10.1007/978-3-662-45201-1\\_3](https://doi.org/10.1007/978-3-662-45201-1_3).
- Bosworth, W., Burke, K., 2005. Evolution of the Red Sea—Gulf of Aden rift system. In: *Petroleum Systems of Divergent Continental Margin Basins: 25th Annual*, pp. 342–372. <https://doi.org/10.5724/gcs.05.25.0342>.
- Botz, R., Schmidt, M., Wehner, H., Hufnagel, H., Stoffers, P., 2007. Organic-rich sediments in brine-filled Shaban- and Kebrit deeps, northern Red Sea. *Chem. Geol.* 244 (3), 520–553. <https://doi.org/10.1016/j.chemgeo.2007.07.004>.
- Bristow, T.F., Grotzinger, J.P., Rampe, E.B., Cuadros, J., Chipera, S.J., Downs, G.W., Fedo, C.M., Frydenvang, J., McAdam, A.C., Morris, R.V., Achilles, C.N., Blake, D.F., Castle, N., Craig, P., Des Marais, D.J., Downs, R.T., Hazen, R.M., Ming, D.W., Morrison, S.M., Vasavada, A.R., 2021. Brine-driven destruction of clay minerals in Gale Crater. *Mar. Sci.* 373 (6551), 198–204. <https://doi.org/10.1126/science.abg5449>.
- Camerlenghi, A., 1990. Anoxic basins of the eastern mediterranean: Geological Framework. *Mar. Chem.* 31 (1–3), 1–19. [https://doi.org/10.1016/0304-4203\(90\)90028-b](https://doi.org/10.1016/0304-4203(90)90028-b).
- Canfield, D.E., Farquhar, J., 2009. Animal evolution, bioturbation, and the sulfate concentration of the oceans. *Proc. Natl. Acad. Sci.* 106 (20), 8123–8127. <https://doi.org/10.1073/pnas.0902037106>.
- Censi, P., Raso, M., Saiano, F., Zuddas, P., Oliveri, E., 2019. Zr/Hf ratio and REE behaviour: a coupled indication of lithogenic input in marginal basins and deep-sea brines. *Deep-Sea Res. II Top. Stud. Oceanogr.* 164, 216–223.
- Chalastani, V.I., Manatos, P., Al-Suwailem, A.M., Hale, J.A., Vijayan, A.P., Pagano, J., Williamson, I., Henshaw, S.D., Albaset, R., Butt, F., Brainard, R.E., Coccossis, H., Tsoukala, V.K., Duarte, C.M., 2020. Reconciling tourism development and conservation outcomes through marine spatial planning for a saudi Giga-Project in

- the Red Sea (The Red Sea Project, Vision 2030). *Front. Mar. Sci.* 7. <https://doi.org/10.3389/fmars.2020.00168>.
- Cita, M.B., 1991. Anoxic basins of the eastern mediterranean: an overview. *Paleoceanography* 6 (1), 133–141. <https://doi.org/10.1029/90pa01789>.
- Cita, M.B., 2006. Exhumation of Messinian evaporites in the deep-sea and creation of deep anoxic brine-filled collapsed basins. *Sediment. Geol.* 188–189, 357–378. <https://doi.org/10.1016/j.sedgeo.2006.03.013>.
- Cochran, J.R., Martinez, F., Steckler, M.S., Hobart, M.A., 1986. Conrad deep: a new northern Red Sea deep. *Earth Planet. Sci. Lett.* 78 (1), 18–32. [https://doi.org/10.1016/0012-821x\(86\)90169-x](https://doi.org/10.1016/0012-821x(86)90169-x).
- Coleman, R.G., 1993. *Geologic Evolution of the Red Sea*. Oxford University Press.
- Craig, H., 1969. Geochemistry and origin of the Red Sea brines. In: Degens, E.T., Ross, D. A. (Eds.), *Hot Brines and Recent Heavy Metal Deposits in the Red Sea: A Geochemical and Geophysical Account*. Springer Berlin Heidelberg, Berlin, Heidelberg, pp. 208–242.
- Cramer, W., Guiot, J., Fader, M., Garrabou, J., Gattuso, J.P., Iglesias, A., Lange, M.A., Lionello, P., Llasat, M.C., Paz, S., Peñuelas, J., Snoussi, M., Toreti, A., Tsimplis, M.N., Xoplaki, E., 2018. Climate change and interconnected risks to sustainable development in the Mediterranean. *Nat. Clim. Chang.* 8, 972–980.
- Decampo, D.M., Jones, B.F., 2014. Geochemistry of saline lakes. In: *Treatise on Geochemistry*, pp. 437–469. <https://doi.org/10.1016/b978-0-08-095975-7.00515-5>.
- Dickens, G.R., Koelling, M., Smith, D.C., Schnieders, L., 2007. Rhizon sampling of pore waters on scientific drilling expeditions: an example from the IODP Expedition 302, Arctic Coring Expedition (Acex). *Sci. Drill.* 4, 22–25. <https://doi.org/10.5194/sd-4-22-2007>.
- Dickson, A.G., Afghan, J.D., Anderson, G.C., 2003. Reference materials for oceanic CO<sub>2</sub> analysis: a method for the certification of total alkalinity. *Mar. Chem.* 80, 185–197.
- Duarte, C.M., Røstad, A., Michoud, G., Barozzi, A., Merlini, G., Delgado-Huertas, A., Hession, B.C., Mallon, F.L., Afifi, A.M., Daffonchio, D., 2020. Discovery of Afifi, the shallowest and southernmost brine pool reported in the Red Sea. *Sci. Rep.* 10 (1), 910. <https://doi.org/10.1038/s41598-020-57416-w>.
- Dundas, I., 1998. Was the environment for primordial life hypersaline? *Extremophiles* 2 (3), 375–377. <https://doi.org/10.1007/s007920050081>.
- English, P.M., 2001. Formation of analcime and moganite at Lake Lewis, Central Australia: significance of groundwater evolution in diagenesis. *Sediment. Geol.* 143 (3–4), 219–244. [https://doi.org/10.1016/s0037-0738\(01\)00063-x](https://doi.org/10.1016/s0037-0738(01)00063-x).
- Esau, L., Zhang, G., Sagar, S., Stingl, U., Bajic, V.B., Kaur, M., 2019. Mining the deep red-sea brine pool microbial community for anticancer therapeutics. *BMC Complement. Altern. Med.* 19 (1) <https://doi.org/10.1186/s12906-019-2554-0>.
- Fisher, L.A., Pontefract, A., Som, S., Carr, C.E., Klempay, B., Schmidt, B., Bowman, J., Bartlett, D.H., 2021. Current state of athalassohaline deep-sea hypersaline anoxic basin research—recommendations for future work and relevance to astrobiology. *Environ. Microbiol.* 23 (7), 3360–3369. <https://doi.org/10.1111/1462-2920.15414>.
- Gieskes, J.M., Gamo, T., Brumsack, H., 1991. Chemical methods for interstitial water analysis aboard JOIDES resolution. In: *Technical Notes. Ocean Drilling Program*, Texas A&M, College Station.
- Goodman Tchernov, B., Katz, T., Shaked, Y., Qupty, N., Kanari, M., Niemi, T., Agnon, A., 2016. Offshore evidence for an undocumented tsunami event in the 'low risk' Gulf of Aqaba-Eilat, Northern Red Sea. *PLoS One* 11 (1), e0145802.
- Gran, G., 1950. Determination of the equivalence point in potentiometric titrations. *Acta Chem. Scand.* 4, 559–577.
- Gurvich, E.G., 2006. *Metalliferous Sediments of the World Ocean: Fundamental Theory of Deep-sea Hydrothermal Sedimentation*. Springer.
- Harouaka, K., Allen, C., Bylaska, E., Cox, R.M., Eiden, G.C., di Vacri, M.R., Hoppe, E.W., Arnquist, I.J., 2021. Gas-phase ion-molecule interactions in a collision reaction cell with triple quadrupole-inductively coupled plasma mass spectrometry: investigations with N<sub>2</sub>O as the reaction gas. *Spectrochim. Acta B At. Spectrosc.* 186, 106309.
- Hartmann, M., Scholten, J.C., Stoffers, P., Wehner, F., 1998. Hydrographic structure of brine-filled deeps in the Red Sea—new results from the Shaban, KEBRIT, Atlantis II, and Discovery Deep. *Mar. Geol.* 144 (4), 311–330. [https://doi.org/10.1016/s0025-3227\(97\)00055-8](https://doi.org/10.1016/s0025-3227(97)00055-8).
- Herut, B., Rubin-Blum, M., Sisma-Ventura, G., Jacobson, Y., Bialik, O.M., Ozer, T., Lawal, M.A., Giladi, A., Kanari, M., Antler, G., Makovsky, Y., 2022. Discovery and chemical composition of the eastmost deep-sea anoxic brine pools in the Eastern Mediterranean Sea. *Front. Mar. Sci.* 9, 1040681.
- Horikoshi, K., 1998. Barophiles: deep-sea microorganisms adapted to an extreme environment. *Curr. Opin. Microbiol.* 1 (3), 291–295.
- Hughes, G.W., Beydoun, Z.R., 1992. The Red Sea — Gulf of Aden: biostratigraphy, lithostratigraphy and palaeoenvironments. *J. Pet. Geol.* 15 (s3), 135–156. <https://doi.org/10.1111/j.1747-5457.1992.tb00959.x>.
- Hunt, J.M., Hays, E.E., Degens, E.T., Ross, D.A., 1967. Red Sea: detailed survey of hot-brine areas. *Science* 156 (3774), 514–516. <https://doi.org/10.1126/science.156.3774.514>.
- Ibrahim, A.M.M., Abdelmenam, M.A., 2013. Heavy metals in Suez Canal and Red Sea gulfs, review article. *Blue Biotechnol. J.* 2 (1), 51–77.
- Javaux, E.J., 2006. Extreme life on Earth—past, present and possibly beyond. *Res. Microbiol.* 157 (1), 37–48.
- Javor, B., Javor, B., 1989. Solar salters. *Hypersaline Environ. Microbiol. Biogeochemistry* 189–204.
- Joye, S.B., 2020. The geology and biogeochemistry of hydrocarbon seeps. *Annu. Rev. Earth Planet. Sci.* 48 (1), 205–231. <https://doi.org/10.1146/annurev-earth-063016-020052>.
- Joye, S.B., MacDonald, I.R., Montoya, J.P., Peccini, M., 2005. Geophysical and geochemical signatures of Gulf of Mexico seafloor brines. *Biogeosciences* 2 (3), 295–309. <https://doi.org/10.5194/bg-2-295-2005>.
- Kalman, A., Katz, T., Hill, P., Goodman-Tchernov, B., 2020. Droughts in the desert: Medieval Warm Period associated with coarse sediment layers in the Gulf of Aqaba-Eilat, Red Sea. *Sedimentology* 67 (6), 3152–3166. <https://doi.org/10.1111/sed.12737>.
- Kanari, M., Ben-Avraham, Z., Tibor, G., Bookman, R., Goodman-Tchernov, B., Niemi, T., Wechsler, N., Ash, A., Taha, N., Marco, S., 2015. On-land and offshore evidence for Holocene earthquakes in the Northern Gulf of Aqaba-Elat, Israel/Jordan. *Miscellanea INGV* 27, 240–243.
- Karbe, L., 1987. In: Edwards, A.J., Head, S.M. (Eds.), *Hot Brines and the Deep Sea Environment*. Pergamon Press, Oxford, pp. 70–89.
- Katz, T., Ginat, H., Eyal, G., Steiner, Z., Braun, Y., Shalev, S., Goodman-Tchernov, B.N., 2015. Desert flash floods form hyperpycnal flows in the coral-rich Gulf of Aqaba, Red Sea. *Earth Planet. Sci. Lett.* 417, 87–98. <https://doi.org/10.1016/j.epsl.2015.02.025>.
- Knauth, L.P., 1998. Salinity history of the Earth's early ocean. *Nature* 395 (6702), 554–555. <https://doi.org/10.1038/26879>.
- Knauth, L.P., 2005. Temperature and salinity history of the Precambrian Ocean: implications for the course of microbial evolution. *Palaeogeogr. Palaeoclimatol. Palaeoecol.* 219 (1–2), 53–69. <https://doi.org/10.1016/j.palaeo.2004.10.014>.
- Knight, B.P., Chaudri, A.M., McGrath, S.P., Giller, K.E., 1998. Determination of chemical availability of cadmium and zinc in soils using inert soil moisture samplers. *Environ. Pollut.* 99 (3), 293–298. [https://doi.org/10.1016/s0269-7491\(98\)00021-9](https://doi.org/10.1016/s0269-7491(98)00021-9).
- Knoll, A.H., 2015. *Life on a Young Planet: The First Three Billion Years of Evolution on Earth*. Princeton University Press. <https://doi.org/10.1515/9781400866045>.
- Larsen, D., 2008. Revisiting silicate Authigenesis in the pliocene–pleistocene lake tecopa beds, southeastern California: depositional and hydrological controls. *Geosphere* 4 (3), 612. <https://doi.org/10.1130/ges00152.1>.
- Lee, O.O., Wang, Y., Tian, R., Zhang, W., Shek, C.S., Bougouffa, S., Al-Suwailem, A., Batang, Z.B., Xu, W., Wang, G.C., Zhang, X., 2014. In situ environment rather than substrate type dictates microbial community structure of biofilms in a cold seep system. *Sci. Rep.* 4 (1), 3587.
- MacDonald, I.R., Reilly, J.F., Guinasso, N.L., Brooks, J.M., Carney, R.S., Bryant, W.A., Bright, T.J., 1990. Chemosynthetic mussels at a brine-filled pockmark in the northern Gulf of Mexico. *Science* 248 (4959), 1096–1099. <https://doi.org/10.1126/science.248.4959.1096>.
- Mackenzie, F.T., Andersson, A.J., 2011. Biological control on diagenesis: influence of bacteria and relevance to ocean acidification. In: Reitner, J., Thiel, V. (Eds.), *Encyclopedia of Geobiology, Encyclopedia of Earth Sciences Series*. Springer, Dordrecht. [https://doi.org/10.1007/978-1-4020-9212-1\\_73](https://doi.org/10.1007/978-1-4020-9212-1_73).
- Macumber, P.G., 1992. Hydrological processes in the Tyrrell Basin, southeastern Australia. *Chem. Geol.* 96 (1–2), 1–18. [https://doi.org/10.1016/0009-2541\(92\)90118-o](https://doi.org/10.1016/0009-2541(92)90118-o).
- Mancinelli, R.L., Fahlen, T.F., Landheim, R., Klovstad, M.R., 2004. Brines and evaporates: analogs for martian life. *Adv. Space Res.* 33 (8), 1244–1246. <https://doi.org/10.1016/j.asr.2003.08.034>.
- Martin, J.B., 1994. Diagenesis and hydrology and the New Hebrides forearc and intra-arc Aoba Basin. In: Green, H.G., et al. (Eds.), *Pro. Ocean Drill. Program, 134 Sci. Results*, vol. 134, pp. 109–130.
- McGuire, A.V., Bohannon, R.G., 1989. Timing of mantle upwelling: evidence for a passive origin for the Red Sea Rift. *J. Geophys. Res.* 94 (B2), 1677. <https://doi.org/10.1029/jb094i0b02p01677>.
- Michaelis, W., Jenisch, A., Richnow, H.H., 1990. Hydrothermal petroleum generation in Red Sea sediments from the Kebrit and Shaban Deeps. *Appl. Geochem.* 5 (1–2), 103–114.
- Miller, A.R., Densmore, C.D., Degens, E.T., Hathaway, J.C., Manheim, F.T., McFarlin, P. F., Pocklington, R., Jokela, A., 1966. Hot brines and recent iron deposits in deeps of the Red Sea. *Geochim. Cosmochim. Acta* 30 (3), 341–359. [https://doi.org/10.1016/0016-7037\(66\)90007-x](https://doi.org/10.1016/0016-7037(66)90007-x).
- Pätzold, J., Halbach, P.E., Hempel, G., Weikert, H., 2000. Eastern Mediterranean—Northern Red Sea 1999, Cruise No. 44, 22 January–16 May 1999. METEOR-Berichte, Universität Hamburg.
- Pätzold, J., Bohrmann, G., Hübscher, C., 2003. Black Sea—Mediterranean—Red Sea, Cruise No. 52, January 2–March 27, 2002. METEOR-Berichte, Universität Hamburg.
- Pautot, G., Guennoc, P., Coutelle, A., Lyberis, N., 1984. Discovery of a large brine pool in the northern Red Sea. *Nature* 310 (5973), 133–136.
- Pierret, M.C., Clauer, N., Bosch, D., Blanc, G., France-Lanord, C., 2001. Chemical and isotopic (<sup>87</sup>Sr/<sup>86</sup>Sr, <sup>81</sup>O, δD) constraints on the formation processes of Red-Sea brines. *Geochim. Cosmochim. Acta* 65 (8), 1259–1275.
- Purkis, S.J., Harris, P.M.M., Ellis, J., 2012. Patterns of sedimentation in the contemporary Red Sea as an analog for ancient carbonates in rift settings. *J. Sediment. Res.* 82 (11), 859–870.
- Purkis, S.J., Shernisky, H., Swart, P.K., Sharifi, A., Oehlert, A., Marchese, F., Benzoni, F., Chimienti, G., Duchatellier, G., Klaus, J., Eberli, G.P., 2022a. Discovery of the deep-sea NEOM Brine Pools in the Gulf of Aqaba, Red Sea. *Commun. Earth Environ.* 3 (1), 146.
- Purkis, S.J., Ward, S.N., Shernisky, H., Chimienti, G., Sharifi, A., Marchese, F., Benzoni, F., Rodrique, M., Raymo, M.E., Abdulla, A., 2022b. Tsunamigenic potential of an incipient submarine landslide in the Tiran Straits. *Geophys. Res. Lett.* 49 (4), e2021GL097493.
- Reyensbach, A.L., Cady, S.L., 2001. Microbiology of ancient and modern hydrothermal systems. *Trends Microbiol.* 9 (2), 79–86. [https://doi.org/10.1016/s0966-842x\(00\)01921-1](https://doi.org/10.1016/s0966-842x(00)01921-1).

- Rimoldi, B., 1993. Turbiditic sediments in anoxic environments of the eastern Mediterranean: core KCO6B (Lebeccio Basin). Preliminary results. *Rend. Fis. Acc. Lincei.* 4 (9), 237–248.
- Rimoldi, B., Alexander, J., Morris, S., 1996. Experimental turbidity currents entering density-stratified water: analogues for turbidites in Mediterranean hypersaline basins. *Sedimentology* 43, 527–540. <https://doi.org/10.1046/j.1365-3091.1996.d01-21.x>.
- Ross, D.A., Hunt, J.M., 1967. Third brine pool in the Red Sea. *Nature* 213 (5077), 687–688. <https://doi.org/10.1038/213687a0>.
- Rothschild, L.J., Mancinelli, R.L., 2001. Life in extreme environments. *Nature* 409 (6823), 1092–1101.
- Salamon, A., Frucht, E., Ward, S.N., Gal, E., Grigorovitch, M., Shem-Tov, R., Calvo, R., Ginat, H., 2021. Tsunami hazard evaluation for the head of the Gulf of Elat–Aqaba, Northeastern Red Sea. *Front. Earth Sci.* 8 <https://doi.org/10.3389/feart.2020.602462>.
- Salem, E.-S.M., 2009. Paleo-tsunami deposits on the Red Sea beach, Egypt. *Arab. J. Geosci.* 2 (2), 185–197. <https://doi.org/10.1007/s12517-008-0027-8>.
- Salem, M., 2017. Study of Conrad and Shaban Deep Brines, Red Sea, using bathymetric, parsound and seismic surveys. *NRIAG J. Astron. Geophys.* 6 (1), 90–96. <https://doi.org/10.1016/j.nrjag.2017.04.003>.
- Sawyer, D.E., Mason, R.A., Cook, A.E., Portnov, A., 2019. Submarine landslides induce massive waves in subsea brine pools. *Sci. Rep.* 9, 128.
- Schmidt, M., Botz, R., Faber, E., Schmitt, M., Poggenburg, J., Garbe-Schönberg, D., Stoffers, P., 2003. High-resolution methane profiles across anoxic brine–seawater boundaries in the Atlantis-II, Discovery, and Kebrat Deeps (Red Sea). *Chem. Geol.* 200 (3–4), 359–375. [https://doi.org/10.1016/s0009-2541\(03\)00206-7](https://doi.org/10.1016/s0009-2541(03)00206-7).
- Schmidt, M., Devey, C., Eisenhauer, A., 2011. FS Poseidon Fahrbericht/Cruise Report P408—The Jeddah Transect; Jeddah—Jeddah, Saudi Arabia, 13.01.–02.03.2011 IFM-GEOMAR Report 46. IFM-GEOMAR, Kiel.
- Schardt, C., 2016. Hydrothermal fluid migration and brine pool formation in the Red Sea: the Atlantis II Deep. *Mineral. Deposita* 51 (1), 89–111. <https://doi.org/10.1007/s00126-015-0583-2>.
- Schmidt, M., Al-Farawati, R., Al-Aidaroos, A., Kürten, B., 2013. RV PELAGIA Fahrbericht/Cruise Report 64PE350/64PE351—JEDDAH-TRANSECT; 08.03.–05.04.2012 Jeddah-Jeddah, 06.04–22.04.2012 Jeddah-Duba. GEOMAR Report, N. Ser. 005. GEOMAR Helmholtz Centre for Ocean Research, Kiel. [https://doi.org/10.3289/GEOMAR\\_REP\\_NS\\_5\\_2013](https://doi.org/10.3289/GEOMAR_REP_NS_5_2013).
- Schmidt, M., Al-Farawati, R., Botz, R., 2015. Geochemical classification of brine-filled Red Sea deeps. In: The Red Sea, pp. 219–233. [https://doi.org/10.1007/978-3-662-45201-1\\_13](https://doi.org/10.1007/978-3-662-45201-1_13).
- Schoell, M., Faber, E., 1978. New isotopic evidence for the origin of Red Sea brines. *Nature* 275 (5679), 436–438. <https://doi.org/10.1038/275436a0>.
- Scholten, J.C., Staffers, P., Garbe-Schönberg, D., Moammar, M., 2000. Hydrothermal mineralization in the Red Sea. In: Handbook of Marine Mineral Deposits, pp. 369–395. <https://doi.org/10.1201/9780203752760-14>.
- Seeberg-Elverfeldt, J., Schlüter, M., Feseker, T., Kölling, M., 2005. Rhizon sampling of porewaters near the sediment-water interface of aquatic systems. *Limnol. Oceanogr. Methods* 3 (8), 361–371. <https://doi.org/10.4319/lom.2005.3.361>.
- Shaked, Y., Agnon, A., Lazar, B., Marco, S., Avner, U., Stein, M., 2004. Large earthquakes kill coral reefs at the north-west Gulf of Aqaba. *Terra Nova* 16 (3), 133–138. <https://doi.org/10.1111/j.1365-3121.2004.00541.x>.
- Shokes, R.F., Trabant, P.K., Presley, B.J., Reid, D.F., 1977. Anoxic, hypersaline basin in the northern Gulf of Mexico. *Science* 196 (4297), 1443–1446. <https://doi.org/10.1126/science.196.4297.1443>.
- Stanley, D.J., Maldonado, A., 1981. Depositional models for fine-grained sediment in the western Hellenic Trench, Eastern Mediterranean. *Sedimentology* 28 (2), 273–290.
- Stockli, D.F., Bosworth, W., 2018. Timing of extensional faulting along the magma-poor central and northern Red Sea Rift margin—transition from regional extension to necking along a hyperextended rifted margin. In: Geological Setting, Palaeoenvironment and Archaeology of the Red Sea, pp. 81–111. [https://doi.org/10.1007/978-3-319-99408-6\\_5](https://doi.org/10.1007/978-3-319-99408-6_5).
- Stoeck, T., Filker, S., Edgcomb, V., Orsi, W., Yakimov, M.M., Pachiadaki, M., Breiner, H.-W., LaCono, V., Stock, A., 2014. Living at the limits: evidence for microbial eukaryotes thriving under pressure in deep anoxic, hypersaline habitats. *Adv. Ecol.* 2014, 1–9. <https://doi.org/10.1155/2014/532687>.
- Stoffers, P., Kühn, R., 1974. Red Sea evaporates: a petrographic and geochemical study. *Initial Rep. Deep Sea Drill. Proj.* 23 <https://doi.org/10.2973/dsdp.proc.23.122.1974>.
- Swallow, J.C., Crease, J., 1965. Hot salty water at the bottom of the Red Sea. *Nature* 205 (4967), 165–166. <https://doi.org/10.1038/205165a0>.
- Swart, P.K., Kramer, P.A., 1998. Geology of mud islands in Florida Bay. In: Vacher, H.L., Quinn, T. (Eds.), *The Hydrology of Carbonate Islands*. Elsevier.
- Torres, M.E., Marsaglia, K.M., Martin, J.B., Murry, R.W., 1995. Sediment diagenesis in western Pacific Basins. In: Taylor, B., Natland, J. (Eds.), *Active Margins and Marginal Basins of the Western Pacific*, AGU Geophysical Monograph Series, vol. 88, pp. 241–258.
- Trüper, H.G., 1969. Bacterial sulfate reduction in the Red Sea hot brines. In: *Hot brines and recent heavy metal deposits in the Red Sea: a geochemical and geophysical account*, pp. 263–271.
- van der Wielen, P.W., Bolhuis, H., Borin, S., Daffonchio, D., Corselli, C., Giuliano, L., D'Auria, G., de Lange, G.J., Huebner, A., Varnavas, S.P., Thomson, J., Tamburini, C., Marty, D., McGinity, T.J., Timmis, K.N., 2005. The enigma of prokaryotic life in deep hypersaline anoxic basins. *Science* 307 (5706), 121–123. <https://doi.org/10.1126/science.1103569>.
- Vengosh, A., Starinsky, A., 1993. Relics of evaporated sea water in deep basins of the eastern Mediterranean. *Mar. Geol.* 115 (1–2), 15–19.
- Vengosh, A., De Lange, G.J., Starinsky, A., 1998. Boron isotope and geochemical evidence for the origin of Urania and Bannock brines at the eastern Mediterranean: effect of water-rock interactions. *Geochim. Cosmochim. Acta* 62 (19–20), 3221–3228.
- Wallmann, K., Suess, E., Westbrook, G.H., Winckler, G., Cita, M.B., 1997. Salty brines on the Mediterranean Sea floor. *Nature* 387 (6628), 31–32. <https://doi.org/10.1038/387031a0>.
- Westbrook, G.K., Reston, T.J., 2002. The accretionary complex of the Mediterranean Ridge: tectonics, fluid flow and the formation of Brine Lakes – an introduction to the special issue of Marine Geology. *Mar. Geol.* 186 (1–2), 1–8. [https://doi.org/10.1016/s0025-3227\(02\)00169-x](https://doi.org/10.1016/s0025-3227(02)00169-x).
- Yakimov, M.M., La Cono, V., Slepak, V.Z., La Spada, G., Arcadi, E., Messina, E., Borghini, M., Monticelli, L.S., Rojo, D., Barbas, C., Golysheva, O.V., Ferrer, M., Golyshev, P.N., Giuliano, L., 2013. Microbial life in the Lake Medee, the largest deep-sea salt-saturated formation. *Sci. Rep.* 3 (1) <https://doi.org/10.1038/srep03554>.
- Zhang, Z., 2020. Rapid shifts in chemical and isotopic compositions of sediment pore waters in the Amami Sankaku Basin in response to initial arc rifting in the mid-Oligocene. *Geochim. Geophys. Geosyst.* 21 (3), e2019GC008845.
- Zierenberg, R.A., Shanks III, W.C., 1986. Isotopic constraints on the origin of the Atlantis II, Suakin and Valdivia brines, Red Sea. *Geochim. Cosmochim. Acta* 50 (10), 2205–2214.
- Ziko, L., Adel, M., Malash, M.N., Siam, R., 2019. Insights into Red Sea brine pool specialized metabolism gene clusters encoding potential metabolites for biotechnological applications and extremophile survival. *Mar. Drugs* 17 (5), 273. <https://doi.org/10.3390/md17050273>.